Himmelfarb Health Sciences Library, The George Washington University Health Sciences Research Commons

Urology Faculty Publications

Urology

2017

H-IPSE is a pathogen-secreted host nucleus infiltrating protein (infiltrin) 3 expressed exclusively by the Schistosoma haematobium egg stage

Luke Pennington

Abdulaziz Alouffi

Evaristus Mbanefo

Debalina Ray

David Heery

See next page for additional authors

Follow this and additional works at: https://hsrc.himmelfarb.gwu.edu/smhs_uro_facpubs Part of the <u>Parasitic Diseases Commons</u>, <u>Parasitology Commons</u>, and the <u>Urology Commons</u>

APA Citation

Pennington, L., Alouffi, A., Mbanefo, E., Ray, D., Heery, D., Jardetzky, T., Hsieh, M., & Falcone, F. (2017). H-IPSE is a pathogensecreted host nucleus infiltrating protein (infiltrin) 3 expressed exclusively by the Schistosoma haematobium egg stage. *Infection and Immunity*, (). http://dx.doi.org/10.1128/IAI.00301-17

This Journal Article is brought to you for free and open access by the Urology at Health Sciences Research Commons. It has been accepted for inclusion in Urology Faculty Publications by an authorized administrator of Health Sciences Research Commons. For more information, please contact hsrc@gwu.edu.

Authors

Luke Pennington, Abdulaziz Alouffi, Evaristus Mbanefo, Debalina Ray, David Heery, Theodore Jardetzky, Michael Hsieh, and Franco Falcone

IAI Accepted Manuscript Posted Online 18 September 2017 Infect. Immun. doi:10.1128/IAI.00301-17 Copyright © 2017 Pennington et al. This is an open-access article distributed under the terms of the Creative Commons Attribution 4.0 International license.

1 <u>TITLE</u>

- 2 H-IPSE is a pathogen-secreted host nucleus infiltrating protein (infiltrin)
- 3 expressed exclusively by the Schistosoma haematobium egg stage

4 RUNNING TITLE

5 H-IPSE nuclear infiltrin from *Schistosoma haematobium*

6 <u>AUTHORS</u>

- 7 Luke F. Pennington^{a\$}, Abdulaziz Alouffi^{b\$} Evaristus C. Mbanefo^c, Debalina Ray^d,
- 8 David M. Heery^e, Theodore S. Jardetzky^a, Michael H. Hsieh^{c,f} and Franco H.
- 9 Falcone^b
- 10 ^{\$} Equal contributors
- 11 AFFILIATIONS
- ¹² ^aStanford University School of Medicine, Stanford, CA, USA;
- 13 ^bSchool of Pharmacy, Division of Molecular Therapeutics and Formulation,
- 14 University of Nottingham, Nottingham, UK;
- 15 ^c Biomedical Research Institute, Rockville, MD, USA
- ¹⁶ ^dDepartment of Pathology, University of California, San Francisco, CA,USA
- ¹⁷ ^eSchool of Pharmacy, Division of Biomolecular Science and Medicinal Chemistry,
- 18 University of Nottingham, Nottingham, UK
- ¹⁹ ^fDepartment of Urology, The George Washington University, Washington, D.C., USA

21 CORRESPONDING AUTHOR

- 22 23
- 24 Dr Franco H. Falcone. Mailing address: University of Nottingham, School of
- 25 Pharmacy, Science Road, Boots Science Building, Nottingham, NG7 2RD, United
- 26 Kingdom. Tel: 44 115 84 66073, Fax: 44 115 29 951 5102; E-mail:
- 27 franco.falcone@nottingham.ac.uk

28

29

Downloaded from http://iai.asm.org/ on September 25, 2017 by SERIALS DEPT

30 ABSTRACT

31 Urogenital schistosomiasis, caused by the parasitic trematode Schistosoma 32 haematobium, affects over 112 million people worldwide. As with S. mansoni infections, the pathology in urogenital schistosomiasis is mainly related to the egg 33 stage, which induces granulomatous inflammation of affected tissues. Schistosoma 34 35 eggs and their secretions have been studied extensively for the related S. mansoni organism which is more amenable to laboratory studies. Indeed, we have shown that 36 IPSE/alpha-1 (M-IPSE herein), a major protein secreted from S .mansoni eggs, can 37 38 infiltrate host cells. Although M-IPSE function is unknown, its ability to translocate to their nucleus and bind DNA suggests a possible role in immune modulation of host 39 cell tissues. Whether IPSE homologs are expressed in other Schistosome species 40 41 has not been investigated.

42

Here, we describe the cloning of two paralog genes H03-IPSE and H06-IPSE 43 which are the ortholog of M-IPSE, from the egg-cDNA of S. haematobium. Using 44 PCR and immunodetection, we confirmed that expression of these genes is 45 restricted to the egg stage and female adult worms, while H-IPSE protein is only 46 detectable in mature eggs but not adults. We show that both H03-IPSE and H06-47 IPSE proteins can infiltrate HTB-9 bladder cells when added exogenously to culture 48 medium. Monopartite C-terminal NLS motifs conserved in H03-IPSE 'SKRRRKY' 49 and H06-IPSE 'SKRGRKY' NLS motifs, are responsible for targeting the proteins to 50 the nucleus of HTB-9 cells, as demonstrated by site directed mutagenesis and GFP 51 tagging. Thus, S. haematobium eggs express IPSE homologs that appear to perform 52 53 similar functions in infiltrating host cells.

Downloaded from http://iai.asm.org/ on September 25, 2017 by SERIALS DEPT

55 **INTRODUCTION**

Schistosomes are digenetic blood trematodes, which rely on their egg stage 56 57 for transmission to the intermediate host, a water snail (1). In order to reach the aquatic environment, the eggs deposited by adult female worms in the blood vessels 58 of their mammalian host have to cross several layers of host tissue before they can 59 reach the lumen of the gut, or, in the case of S. haematobium, the bladder. This is a 60 critical step in the life cycle of the parasite and is therefore very likely to have been 61 fine-tuned to the host's immunological and tissue environment during the course of 62 63 evolution. The microenvironment of the bladder and the gut are histologically and immunologically quite different, and this may be reflected in differences between the 64 molecules produced by the eggs of S. haematobium and S. mansoni and the 65 underlying mechanisms leading to translocation of eggs across the tissues. Most 66 proteomic studies have concentrated on the egg stage of the more available 67 trematode, S. mansoni (2-4); these have identified three major protein components 68 (3) produced by mature eggs: omega-1 (5), kappa-5 (6) and IPSE/alpha-1 (7). 69

70

Here, we show that *S. haematobium* expresses multiple variants of a protein homologous to IPSE/alpha-1 in *S. mansoni* (M-IPSE), which we have called H-IPSE, a term which will be used here to collectively describe the different orthologs of M-IPSE in *S. haematobium*. The mRNA expression of H-IPSE is restricted to the egg and female worm stage, but only translated as protein in eggs. H-IPSE shares an important biological activity described for M-IPSE: the ability to be taken up by and translocate to the nucleus of host cells.

78

79

80 MATERIALS AND METHODS

Cloning of IPSE transcripts. Total RNA was isolated from S. haematobium 81 82 eggs from the liver of infected hamsters using TRizol. Following DNAse treatment and inactivation, cDNA was generated from RNA samples using the superscript III 83 first strand cDNA synthesis kit (Invitrogen) with oligo dT primers, or custom oligo dT 84 primers with a 5' anchoring sequence corresponding to 3' RACE reverse primers 85 (See Table S1 in suppl. data). The resulting cDNA was then amplified with either 86 targeted 5' and 3' primers designed from predicted H-IPSE transcripts, or amplified 87 by a nested 3' RACE PCR with a 5' primer targeted to a conserved 5' elements in 88 IPSE using Platinum Taq Supermix (Invitrogen). Gel purified PCR fragments were 89 then treated with Taq polymerase to facilitate cloning into the pCR 2.1-TOPO vector 90 91 included with the TOPO TA cloning kit (Invitrogen) and all positive colonies from the 92 blue/white assay were sequenced.

93

Recombinant protein expression in BL21 Star DE3 E. coli. The H06-IPSE 94 protein coding sequence lacking the N-terminal signal sequence was cloned into the 95 96 pET-100D Topo expression vector (Invitrogen) and transformed into BL21 Star DE3 E. coli. 1L cell cultures were grown to an OD of 0.6 under ampicillin selection (100 97 µg/mL), and were induced with 1mM IPTG for 3 hours before harvest. Cell pellets 98 were then suspended in 50 mL of lysis buffer (6M guanidine hydrochloride, 10 mM 99 imidazole, 20 mM sodium phosphate, and 500 mM NaCl at pH 7.8) and treated with 100 101 EDTA-free protease inhibitor tablets (Pierce). Cells were lysed with three freeze/ thaw cycles and sonicated on ice. Nickel NTA resin purifications were conducted 102 with a binding buffer containing 8M urea, 10 mM imidazole, and PBS at pH 7.4, a 103 wash buffer consisting of 8M urea, 25 mM imidazole, and PBS at a pH of 7.4, and an 104

Infection and Immunity

V

elution buffer containing 8M urea, 300 mM imidazole, and PBS at a pH of 7.4. This
solution was successively dialyzed against PBS pH 7.4 solutions containing 4.0 M,
2.0 M, and 1.0 M urea over three days before being dialyzed overnight against PBS
(see Fig. S4A in suppl. materials). Refolded protein was concentrated to <0.50
mg/mL in a 3.0 kDa cutoff Centricon centrifugal concentrator (EMD Millipore).

Generation of polyclonal IPSE antibodies. Recombinant bacterial derived H06-IPSE protein (obtained as described above) was used to immunize rabbits 4 times over the course of 8 weeks (ProMab Biotechnologies Inc.) (Fig. S1B in suppl. materials). Antibody was precipitated from sera using ammonium sulfate and suspended in PBS with 0.03% sodium azide prior to use.

Cloning of H-IPSE into pTT5 expression vector. To facilitate mammalian 115 expression, codon optimized synthetic IPSE vectors were generated for H03, H06, 116 and M-IPSE (GeneArt Invitrogen). The IPSE variants were PCR amplified from these 117 118 synthetic constructs. A second insert containing the human VEGF signal sequence, 119 an 8x His tag, and a TEV cleavage site was also amplified. These two fragments were inserted into an EcoRI/Nhel-digested pTTVH8G vector (licensed from the 120 121 Canadian Research Council (8)) by Gibson assembly. Subsequently, during vector 122 optimization, the full IPSE expression cassette with N-terminal signal sequence, tag, 123 and cleavage site was transferred from the pTTVH8G vector to the pTT5 vector by 124 conventional restriction cloning using EcoRI and Notl. The H06 SKAAAKY NLS mutant was cloned by site-directed mutagenesis of H06-pTT5 vectors using Phusion 125 126 High Fidelity PCR Master mix (Invitrogen), followed by Dpn1 digestion for 1 hr.

RT-PCR and stage specific expression of H-IPSE. Total RNA was isolated
 from the following *S. haematobium* life cycle stages (obtained from the NIAID
 Schistosomiasis Resource Center for distribution through BEI Resources, NIAID,

NIH): purified eggs, retrieved from the liver of S. haematobium infected hamsters, 130 miracidia, cercariae, schistosomula, adult females, adult males and mixed sex adult 131 132 worms using the RNAzol kit (MRC, Ohio), following the manufacturer's instructions. Contaminating genomic DNA was removed by DNAse treatment using TURBO 133 134 DNase (Invitrogen Ambion, USA) and chemical DNAse inactivation, as per manufacturer's instructions. After removal of genomic DNA contaminants, cDNA was 135 obtained by reverse transcription using iScript cDNA synthesis kit (Bio-Rad, USA) as 136 137 directed by the manufacturer. After reverse transcription, RNA sample concentrations were measured using a Nanodrop ND-1000 spectrophotometer 138 (ThermoScientific Fisher) and adjusted to 500 ng/µL for all samples with molecular 139 grade water. The PCR was performed on a BioRad CFX Connect thermocycler, 140 141 using the following cycling conditions:

Initial denaturation step [2 min at 94 °C], followed by 35 cycles of denaturation [30 142 sec at 94 °C], annealing [45 sec at 56 °C] and extension [1 min at 72 °C], and 143 followed by a final extension [5 min at 72 °C]. The polymerase used was Takara Taq 144 polymerase using 2 µL 10x polymerase buffer, 2 µL 10 µM dNTPs, 1 µL each of 145 (5'-GCTCACTCTCACCACCATG-3') (5'-146 forward and reverse TCCTTCGACGTTTCGATTCAC-3') primers, 2 µL of cDNA template and 11.5 µL 147 molecular grade water in a 20 µL total volume. PCR reactions were then subjected to 148 electrophoretic separation on 1% agarose containing 0.5 µg/mL ethidium bromide in 149 150 0.5x Tris Borate EDTA (TBE) buffer. A 100 bp DNA ladder (Promega, USA) was 151 used for sizing of the amplicon. Gels were imaged using a GelDoc XR Molecular Imager (BioRad, USA) and saved as tif files. The oligonucleotide primers used span 152 153 an intron, discriminating cDNA (295 bp) from genomic DNA (402 bp).

154

155

156 H06-IPSE were recombinantly expressed for uptake and microscopy experiments using the pTT5 HEK293-6E expression platform (L-11565) licensed from the 157 Canadian Research Council (8). A large-scale gene expression workflow was 158 159 developed using 2L vented shaking flasks. Cells were cultivated in suspension in an incubator at 37 °C in 5% CO₂ humidified atmosphere under constant shaking at a 160 rate of 120 rpm. The medium consisted of Freestyle F17 medium (GIBCO, Rockville, 161 MD) supplemented with 0.1% w/v Kolliphor P-188 (Sigma-Aldrich), with 4 mM L-162 glutamine and 25 µg/mL G418 (ThermoScientific Fisher). Freestyle 293 medium 163 (GIBCO, Rockville, MD) was used interchangeably with F17 without glutamine 164 165 supplementation.

Recombinant protein expression using HEK 293-6E cells. H03-IPSE and

166 For transient transfection, 500 mL of cell suspension were mixed with 12.5 mL of medium containing the plasmid DNA and another 12.5 mL of medium for 167 168 resuspension of linear 25 kdA polyethylenimine (PEI) (PolyPlus). The final DNA amount for each pTT construct was 0.5 mg, and this was with mixed 1.5 mg of PEI 169 170 (3:1 PEI:DNA ratio) and incubated for 3 minutes at room temperature. The resultant 171 complex was then added to the cells. 2.5 mL of 20% (w/v) Tryptone N1 (TN1, 172 TekniScience Inc., Canada) was added 24 h after transfection.

173

174 H-IPSE wildtype or mutant proteins, secreted into the HEK293-6E serum-free cell culture medium, were harvested 7 days after transfection, followed by protein 175 176 purification. This supernatant was centrifuged at 2,800 x g for 10 minutes (4° C). 177 followed by 0.22 µm filtration to remove cell debris and aggregates, then purified by 178 immobilized metal affinity chromatography (IMAC) using TALON Superflow cobalt 179 affinity resin (GE Healthcare, Freiburg, Germany) or Ni-NTA Agarose (Qiagen). For

cobalt resin purification the binding buffer consisted of 50 mM sodium phosphate,
300 mM NaCl, pH 7.4; the wash buffer contained 50 mM sodium phosphate, 300 mM
NaCl, 5 mM imidazole, pH 7.4, while the elution buffer consisted of 50 mM sodium
phosphate, 300 mM NaCl 1, 150 mM imidazole, pH 7.4. Nickel resin purifications
were conducted with a binding buffer containing PBS pH 7.4, a wash buffer
consisting of PBS and 10mM imidazole at a pH of 7.4, and an elution buffer
containing PBS and 300mM imidazole at a pH of 7.4.

187

SDS-PAGE, Coomassie stain and Western blotting. 15 µL aliquots of the 188 eluted purified protein fractions were separated by SDS-PAGE using Bio-Rad Mini-189 Protean ready gels (4-20% gradient TGX) in a Mini-Protean electrophoresis cell, as 190 recommended by the manufacturer. The gels were then incubated for half an hour in 191 Instant Blue (Expedeon, Harston, UK) for Coomassie staining, followed by washing 192 in deionised water. For Western Blotting, the gradient TGX gels were transferred to a 193 0.2 µm nitrocellulose membranes using Trans-Blot® Turbo™ Transfer System, as 194 per the manufacturer's protocol (Bio-Rad). The membranes were blocked by 195 blocking buffer (5% (w/v) dried skimmed milk, 0.01% (v/v) Tween 20 and TBS) with 196 197 shaking for 1 hour at room temperature. Next, membranes were incubated with the primary mouse anti-His antibody (GE Healthcare) as primary antibody, which was 198 diluted 1:5000, at 4°C overnight, followed by three washes in Tris-buffered saline 199 200 solution (TBS) containing 1% Tween (T) for 10 minutes each. The membranes were 201 then incubated with anti-mouse IgG (whole molecule), HRP-conjugated antibody 202 (Sigma-Aldrich, UK) as a secondary antibody (1:4000) for one hour at room 203 temperature, followed by washing in the manner described above. Membranes were 204 imaged using a Fuji LAS4000 imager with chemiluminescence-luminol reagent (3 µl

of 30% H₂O₂, Tris/HCl 0.1 mM, pH, 8; 2.5 mM luminol and 400 µM coumaric acid). 205 206 For detection of native IPSE protein in adult worm extract and egg-derived samples 207 approximately 40 µg of parasite-derived material was loaded per well as determined by each samples' A₂₈₀ using a spectrophotometer. These samples were run on 4-208 209 20% ExpressPlus Page gels (Genescript) as directed by manufacturer, and stained with Coomassie Brilliant Blue G250 (BioRad). For western blotting gels were 210 transferred to a 0.22 µm PDVF membrane after preactivation with methanol. The 211 membranes were blocked by blocking buffer (5% (w/v) dried skimmed milk, 0.01% 212 213 (v/v) Tween-20 and PBS) with shaking for 1 hour at room temperature. Next, blots were incubated with polyclonal anti-H06-IPSE rabbit antibodies at a 1:500 dilution 214 and stained overnight at 4°C. After three washes in PBS-T, blots were then 215 developed with polyclonal HRP conjugated goat anti-rabbit secondary antibody 216 (EMD Millipore) at a dilution of 1:5000. The gels were washed 3 additional time in 217 PBS-T and developed with SignalFire ECL reagent (Cell Signaling). 218

219

Cloning of predicted NLS and mutants into pTetra-EGFP. The predicted 220 221 NLS for each protein was subcloned into the Tetra-EGFP vector, which carries a 222 kanamycin resistance gene (9). This vector encodes four EGFP repeats with a multiple cloning site inserted between the third and fourth EGFP sequence. The 223 nucleotides encoding the predicted NLS in H03-IPSE and H06-IPSE, as well as 224 225 predicted NLS mutant and the canonical Sv40 NLS, were inserted into pTetra-EGFP 226 using oligonucleotide primers and specific restriction enzymes (see Table S1 in suppl. mat). This leads to a construct, which codes for a tetra-EFGP fusion protein of 227 228 approximately 113 kDa that due to its large size is completely excluded from the 229 nucleus in the absence of a functional NLS. Initially, 5'-phosphorylated pairs of

 \triangleleft

Infection and Immunity

Accepted Manuscript Posted Online

Infection and Immunity

R

Infection and Immunity

matching oligonucleotides were designed to code putative NLSs containing GATC 230 231 overhangs by using 1 μ L of each oligo (100 μ M) mixed with 98 μ L of 10 mM Tris-HCl, 232 1 mM EDTA, pH 8.0 followed by denaturation at 95°C for 7 minutes, then 3 minutes at 5°C. Next, the double-stranded oligonucleotides and the pTetra-EGFP vector were 233 234 digested with the restriction enzyme Bg/II (New England Biolabs), according to the manufacturer's protocol. The ends of the linearized pTetra-EGFP vector were 235 dephosphorylated with Antarctic Phosphatase (New England BioLabs) to avoid re-236 ligation to itself, following the manufacturer's instructions. Ligation was performed 237 using 1 µL vector, 3 µL insert, 1 µL 10X Buffer T4-ligase, 4 µL molecular biology 238 grade water and 1 U T4 DNA ligase (Promega) in a 10 µL reaction mixture and 239 incubated overnight at 16°C. DNA sequencing (Source BioScience, UK) using T7 240 241 primers determined successful insertion in the correct orientation.

242

HTB-9 Cell culture and transfection. The human bladder cancer cell line 243 HTB-9 (5637 ATCC) was grown in T75 flasks (Sarstedt, Germany) at 37°C in a 244 humidified 5% CO₂ incubator, with Minimum Essential Medium Eagle (MEM; Sigma-245 Aldrich) supplemented with 5% heat-inactivated fetal bovine serum (FBS, GIBCO), 2 246 mM L-glutamine, 100 unit/mL penicillin and 100 µg/mL streptomycin (Sigma-Aldrich, 247 UK). Transient transfections of HTB-9 cells were performed using X-tremeGENE9 248 DNA transfection reagent (Roche Applied Science, Germany) according to the 249 250 manufacturer's protocol. Cells were plated onto 5 mg/mL rat-tail collagen I-coated 251 glass cover slips (Invitrogen, UK, 15mm diameter, # 1 thickness) in 6-well plates, and transfected with the different Tetra-EGFP plasmids at 60-70% confluency. 252

253

A

Cell Fixation and Fluorescence Microscopy. One-day after transfection the 254 cells were washed with Dulbecco's phosphate-buffered saline (DPBS, Gibco) and 255 fixed at room temperature for 10-15 min in 4% paraformaldehyde. The cells were 256 then washed three times with DPBS and incubated with 0.5 g/mL Hoechst 33342 257 stain (Sigma-Aldrich) at room temperature for 8-15 minutes, before washing again 258 three times with DPBS. Slides were mounted with mounting medium (Sigma-259 Aldrich). The transfected cells were visualized by fluorescence microscopy (EVOS fl. 260 Advanced Microscopy Group, USA) or confocal microscopy (LSM510 META, ZEISS, 261 262 Germany), and analyzed using Zeiss LSM Image Browser software (version 263 4.2.0.121).

264

Cellular Uptake of H03-IPSE. HTB9 cells were seeded onto Lab-Tek 8-well 265 chambered cover glass (Nalgene Nunc International) at a density of 5 x 10⁵ cells in 266 order to achieve 50-60% confluency after 24 hours. Cells were then incubated with 267 15-0.40 nM of recombinant proteins (H03-IPSE WT or mut) in serum-free 268 internalization medium (HEPES buffered Ham's F12 medium (SigmaAldrich, UK) 269 containing 10 mM NaHCO₃ and 2 mg/mL (bovine serum albumin) (Fraction V Biomol 270 271 GmbH, Germany), followed by fixation at room temperature for 10-15 min in 4% 272 paraformaldehyde solution. The cells were then washed 4-5 times with DPBS and incubated with 0.5 μg/mL Hoechst 33342 or 5 μM DRAQ5 (Thermo Fisher Scientific) 273 274 nuclear stain for 15 min and permeabilized with 0.2% Triton X-100 in DPBS for 10 275 min. The cells were washed 4-5 times with DPBS and incubated separately at room temperature for 30 min with two different primary antibodies diluted 1:5000, either 276 mouse anti-His antibody (GE Healthcare). The cells were then washed thrice and 277 labelled with the secondary antibody, Alexa Fluor 555-conjugated goat anti-mouse 278

IgG (H+L; Molecular Probes), diluted 1:500 by incubation at room temperature for 30
min, followed by three final washes with DPBS.

281

282 RESULTS

283

284 Identification of H-IPSE variants. To identify homologs of S. mansoni IPSE in 285 the S. haematobium genome, we performed a BLAST search at Wormbase.org using the predicted transcript of M-IPSE (Smp 112110.1) (10-12). This analysis 286 287 identified three paralogs within the S. haematobium genome, all with predicted 288 transcripts with high identity to M-IPSE (Gene ID, % amino acid identity: C_00050, 289 67%: C 00244, 63%: B 00796, 56%). To verify these transcripts we isolated cDNA 290 from S. haematobium eggs, and employed two strategies. The first employed 5' and 291 3' primers designed to amplify transcripts predicted from the C_00244 locus, and the 292 second employed a 3' RACE cloning strategy with a 5' primer targeting highly 293 conserved regions of all H-IPSE variants (Table S1). In total, 14 IPSE transcript 294 sequences were obtained, and 8 Sanger sequencing runs contained data sufficient 295 for unambiguous base calling throughout the ORF's. These transcripts clustered with 296 two of the three H-IPSE paralogs (Figure 1A), and one transcript from each cluster 297 (H03 and H06) was selected for further study. Sequence variations within these 298 clones suggest that H-IPSE genes are polymorphic (see Figures S1-S3 for 299 supplementary information).

300

301 <Figure 1 here>

302

 \triangleleft

Infection and Immunity

Alignment of H03-/H06-IPSE with M-IPSE (Fig. 1B) demonstrates conservation 303 304 of the seven cysteines, known to form three intramolecular disulfide bonds and one 305 intermolecular bond, resulting in a homodimeric structure. Two potential N-linked glycosylation consensus motifs are also present with small variations. A 20 amino 306 307 acid long N-terminal classical secretory sequence (CSS) is predicted for both H03and H06-IPSE by SignalP 4.1 (13). To verify the presence of IPSE protein in S. 308 309 haematobium parasite-derived material, we expressed and refolded H06-IPSE from 310 insoluble inclusion bodies, and used this bacterially derived H06-IPSE to generate 311 polyclonal anti-H-IPSE antibodies in rabbits (Figure S1). On western blots, anti H-IPSE antibodies bind a ~40 kDa protein species in both S. haematobium egg 312 secreted protein and soluble egg antigens, but not in adult worm extract (Figure 1C). 313 314 This corresponds to the expected size for dimeric, glycosylated H-IPSE variants. 315

H03- and H06-IPSE variants have a predicted nuclear localization 316 sequence (NLS). Several algorithms (cNLSMapper (14), pSORTII 317 (15) NLStradamus (16) and NucPred (17)) predict a C-terminal nuclear localization 318 sequence (NLS) in H03-IPSE close to the C-term (data not shown), similarly to the 319 NLS described for M-IPSE (18). Intriguingly, the H06-IPSE paralog carried an 320 321 R128G variant within the nuclear localization sequence corresponding to the validated NLS (18) in M-IPSE (Fig. 1B). Such variants have also been observed in S. 322 323 mansoni studies. For example ESP3-6, a protein later recognized as an M-IPSE 324 variant, is 97% homologous to the published M-IPSE sequence (GenBank Acc. Nr.: AAK26170.1), but contains an R132L variant within the NLS (ESP3-6 GenBank Acc. 325 326 Nr.: AF527011). Positively charged amino acids in an NLS are key to its nuclear 327 targeting activity mediated by binding to cytosolic importin- α (19), thus such a

 $\overline{\triangleleft}$

328

329

330

331

of an NLS in H06-IPSE by cNLSmapper and the other tested algorithms (data not 332 333 shown). 334 The NLS in H03- and H06-IPSE is able to direct a large fluorescent protein 335 336 to the nucleus of mammalian cells. Therefore, in order to assess functionality of the predicted NLS in H03-IPSE and the potential impact of the R128G substitution in 337 H06-IPSE, we cloned the oligonucleotides encoding the NLS predicted sequences 338 into the previously described Tetra-EGFP vector (18). The resulting constructs were 339 then transfected into HTB-9 uroepithelial carcinoma cells as a model of host cells 340 relevant to S. haematobium infection. The results of the transfection of the Tetra-341 EGFP vector encoding the NLS sequences of H03-IPSE (SKRRRKY) and H06-IPSE 342 (SKRGRKY), as well as the predicted NLS mutant SAAGAAY (Figure 2) confirm that 343 the H03-IPSE NLS is fully functional, resulting in complete translocation of the large 344 Tetra-EGFP protein into the nucleus. In the H06-IPSE NLS, the presence of an 345 uncharged G in the charged KRRRK H03-IPSE core sequence of the NLS appears 346 to weaken its strength as nuclear targeting signal, as documented by the mixed 347 cytosolic/nuclear localization in contrast to the exclusive nuclear localization with the 348 349 SKRRRKY H03-IPSE NLS sequence (Fig. 2B). This difference is consistent with the results obtained with different prediction algorithms (not shown). Substitution of 350 351 Lysine and Arginine with Alanine (SAAGAAY) results in a non-functional NLS, which

is no longer able to translocate the Tetra-EGFP protein into the nucleus (Fig. 2A and

replacement will have an impact on the protein's ability to translocate to the nucleus,

ranging from less efficient translocation to no translocation at all, depending on the

exact position in the NLS (19). Substitutions in the NLS will potentially also have an

effect on DNA binding specificity. This is also reflected in the less certain prediction

Downloaded from http://iai.asm.org/ on September 25, 2017 by SERIALS DEPT

352

356

357

358

B). These results clearly show that while the predicted NLS in H03-IPSE is fully 353 functional, the G substitution in the positively charged core compromises this 354 355 function at least in part. Further substitutions almost fully ablate NLS functionality.

Recombinant M-IPSE and H-IPSE can be expressed in high yields in 359 HEK293-6E cells grown in suspension. For subsequent experiments, we cloned 360 and expressed H-IPSE using HEK293-6E cells. This system uses a serum-free 361 medium adapted clone and allows HEK293 cell culture in suspension, enabling high 362 cell densities and recombinant protein yields. Proteins generated using these cells 363 364 are glycosylated, which more closely parallels glycosylation of native proteins. Recombinant protein can be harvested from culture supernatants after transient 365 transfection and can be purified e.g. via IMAC using the 8xHis-Tag in the construct 366 (Figure 3A). 367

368

<Figure 3 here> 369

<Figure 2 here>

370

371 Results shown in Figure 3B demonstrate successful expression of H03-IPSE as a mostly dimeric protein of approximately 38-40 kDa molecular weight, with small 372 amounts of monomeric protein of about 20 kDa, in line with what we have previously 373 374 described for M-IPSE (1,2). The double bands are presumably due to glycosylation variants, which are well described for M-IPSE (21). Purity in eluted fractions after 375 376 IMAC was high, and did not require any additional purification steps for downstream 377 experiments. In our hands, IPSE proteins produced a range of yields, with H03-IPSE

Downloaded from http://iai.asm.org/ on September 25, 2017 by SERIALS DEPT

 \triangleleft

Infection and Immunity

exhibiting the lowest final yield (~5-10 mg/L) and M-IPSE and H06-IPSE SKAAAKY 378 379 NLS mutant producing the highest yield (~15-25 mg/L) (Figure S5). Attempts to 380 concentrate protein to higher concentration above 0.5 mg/mL resulted in formation of aggregates, not seen by SDS, but appearing in size-exclusion chromatography. 381

Recombinant H03-IPSE added exogenously is taken up by HTB-9 382 383 uroepithelial cells and efficiently translocates to the nucleus. To mimic S. haematobium infection conditions, we added recombinant 8xHis tagged H03-IPSE to 384 the culture medium of proliferating HTB-9 uroepithelial carcinoma cells as described 385 386 in Materials and Methods. After 24 hours, fixed cells were immunostained with anti-His tag antibody. As shown in Figure 4, this revealed a highly efficient uptake of 387 exogenous H03-IPSE, which was present in HTB-9 nuclei, as revealed by co-388 staining of nuclear DNA with DRAQ5. The nuclear staining pattern suggests that 389 H03-IPSE was largely excluded from the nucleolar regions. This result indicates that 390 H03-IPSE protein can infiltrate the vast majority of cells with remarkable efficiency 391 and localize to the nucleus. The only cells we observed that did not stain for 392 recombinant H03-IPSE were those actively undergoing mitosis, in which the nuclear 393 membrane is broken down 394

395

396 <Figure 4 here>

397

398 The NLS in H03- and H06-IPSE is essential for nuclear translocation, but 399 not for cellular uptake. Next, we compared the ability of both H-IPSE variants with the ability of the NLS Alanine mutant, to gain access to the nuclear compartment of 400 401 HTB-9 cells when added to cell culture medium. The results, visualized on a 402 fluorescence microscope, are shown in Figure 5. When assessing the subcellular

403 localization of the recombinant molecules with a molecular weight of approximately
404 40 kDa, both H03- and H06-IPSE variants seemed similarly efficient in translocating
405 across the nuclear membrane.

406

407 <Figure 5 here>

408

Unlike what was observed for the Tetra-EGFP-NLS constructs (Fig. 2A and B), 409 we did not find any reduction in translocation efficiency in H06-IPSE compared with 410 H03-IPSE, suggesting that these differences may only become apparent with larger 411 proteins (such as Tetra-EGFP) and thus may not be relevant in the context of 412 molecular crosstalk between H-IPSE and the host cells. In contrast, the SKAAAKY 413 NLS H03 mutant, despite potentially being able to cross nuclear pores due to its low 414 molecular weight, remained completely excluded from the nucleus (Fig. 5 H03-IPSE 415 mut). The H03 mutant appears to be located in vacuoles or endosome-like 416 structures, mainly located around the nucleus, rather than diffuse in the cytoplasm. 417 This suggests that an intact NLS might be an important feature needed e.g. for 418 419 endosomal escape.

The lack of uptake of the Ala mutant shows that the NLS in H-IPSE is monopartite and can be described as necessary and sufficient, i.e. no nuclear translocation occurs in its absence, and it is the only NLS in the molecule. This is consistent with the lack of prediction of additional nuclear translocation signals elsewhere in the molecule. These data also demonstrate that the NLS is not required for H-IPSE transport into cells.

426

H-IPSE mRNA is expressed in S. haematobium adult females and the egg 427 stage. Next, we investigated the expression of H-IPSE across the different life cycle 428 429 stages, using conventional RT-PCR. The results are shown in Figure 6. RT-PCR data indicated adult worm cDNA preparations were more contaminated with genomic 430 431 DNA, in comparison with other life cycles in control experiments; however, DNAse treatment completely removed genomic DNA. Using DNAse-treated samples, RT-432 PCR indicated expression of H-IPSE mRNA in purified eggs, female adult worms 433 434 (AdF), and weak expression in mixed gender adult worms (Ad Mix), but none in 435 cercariae (cer), schistosomula (som), miracidia (mir) or male adult worms (AdM).

<Figure 6 here> 437

438

436

Overall, this result is consistent with an expression pattern restricted to the egg 439 stage (since female worms often contain immature eggs), and similar to what was 440 described for M-IPSE (7). Interestingly, despite the detection of H-IPSE transcripts in 441 AdF, we detected no H-IPSE protein by western blot in AWA preparations (Figure 442 443 1b).

444

445

DISCUSSION 446

The concurrent presence of a classical secretory sequence (CSS) and a 447 nuclear localization sequence (NLS) on the same protein, two apparently 448 contradictory signals in terms of subcellular targeting, is a rare feature. Only four of 449 450 19 tested algorithms correctly identified the presence of a C-terminal, monopartite NLS in H03-IPSE (cNLSmapper (14), PSORT II (15), NLStradamus (16) and 451

Accepted Manuscript Posted Online

Infection and Immunity

NucPred (17)), while most other tested programs predicted a secretory pathway, 452 some unexpectedly also after removal of the signal sequence. Thus prediction of an 453 454 NLS by algorithms is still insufficient and such predictions need to be verified experimentally. At least three properties need to be fulfilled in order to confirm 455 functionality of an NLS; a) a functional NLS needs to be able to direct the protein to 456 457 the nucleus, and b) the NLS in isolation should also be able to direct heterologous proteins to the nucleus. Finally, c) mutation of one or several basic amino acids 458 459 should lead to loss of translocation, or in the case of a single substitution, at least 460 weakening of NLS functionality.

461

462 Our data confirm that the nuclear localization signals present in H03- and H06-463 IPSE are functional and essential for translocation of IPSE into the nuclei of host 464 cells. This is somewhat surprising, as 40 kDa is well below the known limit for 465 passive diffusion across the nuclear pore complex, which has been described as 466 'quite larger than 60 kDa' (23). A possible explanation for such behavior could be yet 467 to be characterized interactions with cellular structures or soluble proteins in the 468 cytosol, making the resulting complex too large for passive diffusion into the nucleus. 469

470 Kosugi and coauthors described six classes of NLS with different specificities 471 for the binding grooves of the karyopherin importin α (19). Based on their 472 classification, the H03-IPSE SKRRRKY would be considered a Class I classical 473 NLS, characterized by a stretch of at least four consecutive basic amino acids (either 474 K or R). In contrast, the SKRGRKY NLS in H06-IPSE conforms with being a Class II 475 classical NLS with the consensus sequence K(K/R)X(K/R), in which one non-basic 476 amino acid interrupts the adjacency of the basic amino acids found in Class I signals,

 $\overline{\triangleleft}$

477 reducing the signal to an interrupted sequence of three basic amino acids. The only difference from Kosugi's predicted canonical patterns is that both H03- and H06-478 479 IPSE appear to possess one additional basic residue in their NLS. Both classes would be predicted to bind to the large major binding pocket of Importin α (19). 480

481

Having shown that the NLS in H-IPSE is fully functional, and bearing in mind 482 that the sequence cannot be functional within the schistosome eggs themselves, as 483 484 the N-terminal CSS will target the protein for secretion well before the N-terminal 485 NLS is synthesized, the key question is what the biological function of such a protein might be. The restriction of its expression to a single stage of the parasitic life cycle 486 (the egg stage), which is in line with the M-IPSE homolog's restricted expression (7), 487 488 suggests a specialized function needed only during a specific phase of egg embryogenesis, or a function needed to govern the very important interaction with 489 the host cells and tissues. The former is unlikely due to the secretory nature of the 490 molecule. To further explore this possibility, we first need to summarize the fate of 491 eggs after oviposition by the female schistosomes. Newly deposited eggs do not 492 have the complex morphology found in mature eggs; this has been described in 493 detail for S. mansoni by Neill (24), Ashton (25), Jurberg (26) and their coauthors. 494 Fewer details are available regarding S. haematobium. Immature eggs are smaller 495 and characterized by the absence of the two envelopes surrounding the miracidia in 496 497 mature eggs: the outer envelope (Reynold's layer, RL) and the inner envelope (von 498 Lichtenberg's layer, vLL). The RL is enriched with tightly packed rough endoplasmic reticulum structures and is therefore thought to be a major site of protein synthesis. 499 500 Under the electron microscope, the RL appears richly surrounded by granular 501 materials in a 1µm wide space underneath the egg shell (25). Eggs deposited in vitro

502 by *ex vivo* worms have been shown to take about a week to fully develop into 503 mature, infective miracidia (27), but development in the host is likely to be more 504 rapid.

The production of the M-IPSE in S. mansoni eggs has been clearly shown to occur in 505 506 the subshell area within the fully formed RL and vLL. This has been demonstrated by 507 immunohistochemical staining with a monoclonal antibody to M-IPSE, and by in situ 508 hybridization with labeled antisense transcripts of full-length M-IPSE cDNA (7). M-509 IPSE can also be seen in contact with the tissues around the eggs (confirming that it 510 is secreted by the eggs) (20) and has been also seen inside surrounding host cells 511 (7). Thus, the emerging picture is that immature eggs initially do not produce IPSE, 512 but that this protein is produced as eggs mature while migrating through the tissues, 513 releasing it into the tissues, where it is able to enter host cells. Inside host cells, it 514 rapidly (in less than half an hour (18)) translocates to the nucleus, where it binds 515 DNA (F. Falcone, unpublished data) with yet-to-be described downstream effects. 516 It is very clear however, that translocation across the host tissues, in order for the eggs to reach the lumen of the bladder or gut, is an event of paramount importance 517 in the life cycle of the parasite. Hence, it can be assumed that molecules secreted 518 519 exclusively by more mature forms of this life stage may be involved in the egress 520 process, and have evolved under high evolutionary pressure.

The first step after oviposition is the escape of eggs from the venules in which they were deposited; *in vitro*, human cells obtained from umbilical venous endothelial cells (HUVECs) rapidly overgrow eggs directly oviposited onto a monolayer (within 4 hours) and a similar behavior is seen when eggs are inserted into umbilical veins (28). More recently, de Walick and coauthors demonstrated deposition of van Willebrand factor and other prothrombic plasma proteins onto the eggshell of *S*.

mansoni (29). However, such steps occur immediately after oviposition, hence IPSE 527 528 and other molecules secreted only after a few days of egg maturation cannot play a 529 role in this initial process. Indeed, it was reported that this process was slower in mature eggs obtained from infected rodent livers in comparison with freshly 530 531 deposited eggs, which may depend on the presence of uterine secretions covering 532 the freshly deposited eggs (28). Once the eggs have reached the perivascular 533 tissues, it takes another few days during which they need to cross several robust 534 layers, including the submucosa, the outer muscularis mucosa, consisting of circular 535 and longitudinal muscle, and the inner mucosa, complete with basal membrane and a very tight epithelial cell layer, before they can reach the lumen. A seemingly 536 537 impossible journey?

538 It is well-accepted that the granulomatous reaction induced by the eggs plays 539 a key role in this process (30, 31); much of the past research has focused on the interactions between immune cells and the schistosome eggs. In S. mansoni, eggs 540 have been proposed to exploit gut lymphoid structures known as Peyer's patches as 541 a preferential route of egress into the gut lumen (32), however a comparable route is 542 not available to S. haematobium in the bladder. This leads to the question whether in 543 addition to the inflammatory granulomatous response involving immune cells, any 544 direct interactions with non-immune cells, such as fibroblasts, muscle cells or 545 epithelial cells are also involved in facilitating egg translocation. In this context, it is 546 interesting to note that in S. haematobium-infected animals, uroplakins and claudins 547 548 involved in epithelial tight junction formation are downregulated after bladder exposure to eggs (33). Whether this downregulation, which is likely to aid egg egress 549 550 by disrupting the integrity of the epithelium is due to the effects of H-IPSE or other egg-derived components, remains to be established. The nuclear translocation and 551

Downloaded from http://iai.asm.org/ on September 25, 2017 by SERIALS DEPT

M

Infection and Immunity

direct effects on gene transcription of H-IPSE are currently under active investigationin our laboratories.

554

Perhaps the most surprising result was to see to what extent an exogenously 555 added parasitic molecule was able to enter host cells. This uptake does not appear 556 557 to be very selective for specific cell types or animal species, as we have seen uptake of M-IPSE in human Huh-7, U2-OS and hamster CHO cell lines (18) as well as 558 HUVEC and human monocyte derived dendritic cells (Falcone et al., unpublished 559 560 data). H-IPSE was taken up by human HTB-9, Huh-7 and monkey Cos-7 cell lines. 561 This raises the question as to whether or which receptors are involved. For M-IPSE, the uptake mechanism has been shown to involve the carbohydrate residues on the 562 563 protein and C-type lectin receptors such as the mannose receptor, the dendritic cellspecific ICAM3-grabbing non-integrin (DC-SIGN), and a macrophage galactose-type 564 lectin and the mannose receptor (34). Similar receptors have been shown to be 565 involved in the uptake of other Schistosome molecules such as omega-1 (5) and 566 kappa-5 (34). Uptake of a secreted molecule by dendritic cells and macrophages has 567 also been shown for S. japonicum Sj16 (35), but there is no information regarding 568 the receptors involved in this process; the expression of Sj16 in E. coli used for the 569 570 described experiments however suggests that protein glycosylation does not play a 571 role in uptake of this molecule.

572

573 Thus secretion of a molecule by a parasitic life stage which is in intimate 574 contact with host tissues, and its subsequent uptake by host cells, may be a more 575 common feature in the host-parasite relationship than hitherto assumed, at least as 576 far as trematodes are concerned. We would like to propose the term 'infiltrin' to

denote the ability of such molecules to enter host cells in the course of crossing 577 several barriers (the cell membrane, presumably the endosomal membrane, and in 578 579 some cases, the nuclear membrane). The archetypal nuclear infiltrins, characterized by the simultaneous presence of a classical secretory and a nuclear localization 580 581 signal (CSS/NLS) signal (11), would be M-IPSE and H-IPSE, while the archetypal cytosolic infiltrin would be omega-1 (5). The ability of exogenous polypeptides to 582 583 enter human cells crossing biological membranes is not a new finding. This was shown for the first time for trans-activating transcriptional activator (TAT) of human 584 585 immunodeficiency virus 1 (HIV-1) in 1988 (36) and the 60 amino acid peptide encoded by antennapedia gene homeobox in Drosophila (37). However, with the 586 exception of our previous report (18), such a principle has not been described for 587 588 molecules secreted by macroparasites, which are too large to enter host cells. HIV-1 Tat can also carry heterologous proteins across the cell membrane (38), a process 589 now understood to be mediated via a caveolin-dependent uptake route (39). 590 Interestingly, both HIV-1 Tat and Drosophila antennapedia homeobox peptide exhibit 591 DNA binding activities, which are also predicted in silico for H-IPSE. Whether H-592 IPSE has similar properties is also under investigation. We believe that these 593 observations make a compelling case warranting more in-depth studies of parasitic 594 595 infiltrins and their potential roles as pathogen-derived nuclear transcription factors.

596

597 Finally, it needs to be noted that H-IPSE's ability to enter host cells is not 598 dependent on an intact NLS, as the H03-IPSE NLS mutant, as well as the previously 599 described M-IPSE NLS mutants (18), are also able to enter mammalian cells. The 500 same is true for HIV-1 Tat, where the regions responsible for cellular uptake and 501 nuclear translocation are distinct (40, 41). Our data suggest that in the absence of an

intact NLS, H-IPSE is able to enter host cells, but remains trapped in endosome-like
vesicles with a perinuclear distribution. Whether NLS mutants retain their ability to
bind host DNA remains to be established.

605

Taken together, we suggests that nuclear infiltrins, by acting e.g. as transcription factors, might play a central role in controlling the host-parasite relationship at the molecular level.

609

610 **REFERENCES**

611

612 1. Gryseels B, Polman K, Clerinx J, Kestens L. 2006. Human schistosomiasis.
613 Lancet 368:1106–18.

Dewalick S, Bexkens ML, van Balkom BWM, Wu Y-P, Smit CH, Hokke CH, de
Groot PG, Heck AJR, Tielens AGM, van Hellemond JJ. 2011. The proteome of
the insoluble *Schistosoma mansoni* eggshell skeleton. Int J Parasitol 41:523–
32.

- Mathieson W, Wilson RA. 2010. A comparative proteomic study of the
 undeveloped and developed *Schistosoma mansoni* egg and its contents: the
 miracidium, hatch fluid and secretions. Int J Parasitol 40:617–28.
- 4. Cass CL, Johnson JR, Califf LL, Xu T, Hernandez HJ, Stadecker MJ, Yates
 JR, Williams DL. 2007. Proteomic analysis of *Schistosoma mansoni* egg
 secretions. Mol Biochem Parasitol 155:84–93.
- 5. Fitzsimmons CM, Schramm G, Jones FM, Chalmers IW, Hoffmann KF,
 Grevelding CG, Wuhrer M, Hokke CH, Haas H, Doenhoff MJ, Dunne DW.
 2005. Molecular characterization of omega-1: A hepatotoxic ribonuclease from

Schistosoma mansoni eggs. Mol Biochem Parasitol 144:123–127.

- 6. Schramm G, Hamilton JV, Balog CIA, Wuhrer M, Gronow A, Beckmann S,
 Wippersteg V, Grevelding CG, Goldmann T, Weber E, Brattig NW, Deelder
 AM, Dunne DW, Hokke CH, Haas H, Doenhoff MJ. 2009. Molecular
 characterisation of kappa-5, a major antigenic glycoprotein from *Schistosoma mansoni* eggs. Mol Biochem Parasitol 166:4–14.
- 633 7. Schramm G, Gronow a, Knobloch J, Wippersteg V, Grevelding CG, Galle J,
 634 Fuller H, Stanley RG, Chiodini PL, Haas H, Doenhoff MJ. 2006. IPSE/alpha-1:
 635 a major immunogenic component secreted from *Schistosoma mansoni* eggs.
 636 Mol Biochem Parasitol 147:9–19.
- 637 8. Delafosse L, Xu P, Durocher Y. 2016. Comparative study of polyethylenimines
 638 for transient gene expression in mammalian HEK293 and CHO cells. J
 639 Biotechnol 227:103–111.

Downloaded from http://iai.asm.org/ on September 25, 2017 by SERIALS DEPT

- Beetz C, Brodhun M, Moutzouris K, Kiehntopf M, Berndt A, Lehnert D, Deufel
 T, Bastmeyer M, Schickel J. 2004. Identification of nuclear localisation
 sequences in spastin (SPG4) using a novel Tetra-GFP reporter system.
 Biochem Biophys Res Commun 318:1079–1084.
- Howe KL, Bolt BJ, Cain S, Chan J, Chen WJ, Davis P, Done J, Down T, Gao
 S, Grove C, Harris TW, Kishore R, Lee R, Lomax J, Li Y, Muller H-M,
 Nakamura C, Nuin P, Paulini M, Raciti D, Schindelman G, Stanley E, Tuli MA,
 Van Auken K, Wang D, Wang X, Williams G, Wright A, Yook K, Berriman M,
 Kersey P, Schedl T, Stein L, Sternberg PW. 2016. WormBase 2016:
 expanding to enable helminth genomic research. Nucleic Acids Res 44:D77480.
- 651 11. Howe KL, Bolt BJ, Shafie M, Kersey P, Berriman M. 2016. WormBase

627

ParaSite - a comprehensive resource for helminth genomics. Mol BiochemParasitol.

Young ND, Jex AR, Li B, Liu S, Yang L, Xiong Z, Li Y, Cantacessi C, Hall RS,
Xu X, Chen F, Wu X, Zerlotini A, Oliveira G, Hofmann A, Zhang G, Fang X,
Kang Y, Campbell BE, Loukas A, Ranganathan S, Rollinson D, Rinaldi G,
Brindley PJ, Yang H, Wang J, Wang J, Gasser RB. 2012. Whole-genome
sequence of *Schistosoma haematobium*. Nat Genet 44:221–5.

13. Petersen TN, Brunak S, von Heijne G, Nielsen H. 2011. SignalP 4.0:
discriminating signal peptides from transmembrane regions. Nat Methods
8:785–786.

Kosugi S, Hasebe M, Tomita M, Yanagawa H. 2009. Systematic identification
of cell cycle-dependent yeast nucleocytoplasmic shuttling proteins by
prediction of composite motifs. Proc Natl Acad Sci U S A 106:10171–10176.

15. Nakai K, Horton P. 1999. PSORT: A program for detecting sorting signals in
 proteins and predicting their subcellular localization. Trends Biochem Sci.

16. Nguyen Ba AN, Pogoutse A, Provart N, Moses AM. 2009. NLStradamus: a
simple Hidden Markov Model for nuclear localization signal prediction. BMC
Bioinformatics 10:202.

Brameier M, Krings A, MacCallum RM. 2007. NucPred - Predicting nuclear
localization of proteins. Bioinformatics 23:1159–1160.

Kaur I, Schramm G, Everts B, Scholzen T, Kindle KB, Beetz C, Montiel-Duarte
C, Blindow S, Jones AT, Haas H, Stolnik S, Heery DM, Falcone FH. 2011.
Interleukin-4-inducing principle from *Schistosoma mansoni* eggs contains a
functional C-terminal nuclear localization signal necessary for nuclear
translocation in mammalian cells but not for its uptake. Infect Immun 79:1779–

 \triangleleft

Infection and Immunity

- Kosugi S, Hasebe M, Matsumura N, Takashima H, Miyamoto-Sato E, Tomita
 M, Yanagawa H. 2009. Six classes of nuclear localization signals specific to
 different binding grooves of importin alpha. J Biol Chem 284:478–85.
- 20. Schramm G, Falcone FH, Gronow A, Haisch K, Mamat U, Doenhoff MJ,
 Oliveira G, Galle J, Dahinden C a, Haas H. 2003. Molecular characterization of
 an interleukin-4-inducing factor from *Schistosoma mansoni* eggs. J Biol Chem
 278:18384–92.
- Wuhrer M, Balog CIA, Catalina MI, Jones FM, Schramm G, Haas H, Doenhoff
 MJ, Dunne DW, Deelder AM, Hokke CH. 2006. IPSE/alpha-1, a major
 secretory glycoprotein antigen from schistosome eggs, expresses the Lewis X
 motif on core-difucosylated N-glycans. FEBS J 273:2276–2292.
- Shatkay H, Höglund A, Brady S, Blum T, Dönnes P, Kohlbacher O. 2007.
 SherLoc: High-accuracy prediction of protein subcellular localization by
 integrating text and protein sequence data. Bioinformatics 23:1410–1417.

Downloaded from http://iai.asm.org/ on September 25, 2017 by SERIALS DEPT

- Wang R, Brattain MG. 2007. The maximal size of protein to diffuse through the
 nuclear pore is larger than 60 kDa. FEBS Lett 581:3164–3170.
- 694 24. Neill PJG, Smith JH, Doughty BL, Kemp M. 1988. The ultrastructure of the
 695 Schistosoma mansoni egg. Am J Trop Med Hyg 39:52–65.
- 696 25. Ashton PDD, Harrop R, Shah B, Wilson RA. 2001. The schistosome egg:
 697 development and secretions. Parasitology 122:329–338.
- Jurberg AD, Gonçalves T, Costa TA, Mattos ACA, Pascarelli BM, Manso PPA,
 Ribeiro-Alves M, Pelajo-Machado M, Peralta JM, Coelho PMZ, Lenzi HL.
 2009. The embryonic development of *Schistosoma mansoni* eggs: Proposal
 for a new staging system. Dev Genes Evol 219:219–234.

- 702 27. Michaels RM, Prata A. 968. Evolution and characteristics of *Schistosoma* 703 mansoni eggs laid in vitro. J Parasitol 54:921–930.
- 704 28. File S. 1995. Interaction of schistosome eggs with vascular endothelium. J
 705 Parasitol 81:234–8.
- deWalick S, Hensbergen PJ, Bexkens ML, Grosserichter-Wagener C, Hokke
 CH, Deelder AM, de Groot PG, Tielens AGM, Van Hellemond JJ. 2014.
 Binding of von Willebrand factor and plasma proteins to the eggshell of *Schistosoma mansoni*. Int J Parasitol 44:263–268.
- 30. Doenhoff MJ, Hassounah O, Murare H, Bain J, Murare H. 1986. The
 schistosome egg granuloma: Immunopathology in the cause of host protection
 or parasite survival? Trans R Soc Trop Med Hyg 80:503–514.
- 713 31. Pearce EJ. 2005. Priming of the immune response by schistosome eggs.
 714 Parasite Immunol.
- Turner JD, Narang P, Coles MC, Mountford AP. 2012. Blood Flukes Exploit
 Peyer's Patch Lymphoid Tissue to Facilitate Transmission from the
 Mammalian Host. PLoS Pathog 8:e1003063.
- 718 33. Ray D, Nelson TA, Fu CL, Patel S, Gong DN, Odegaard JI, Hsieh MH. 2012.
 719 Transcriptional Profiling of the Bladder in Urogenital Schistosomiasis Reveals
 720 Pathways of Inflammatory Fibrosis and Urothelial Compromise. PLoS Negl
 721 Trop Dis 6:e1912.
- 34. Meevissen MHJ, Driessen NN, Smits HH, Versteegh R, van Vliet SJ, van
 Kooyk Y, Schramm G, Deelder AM, Haas H, Yazdanbakhsh M, Hokke CH.
 2012. Specific glycan elements determine differential binding of individual egg
 glycoproteins of the human parasite *Schistosoma mansoni* by host C-type
 lectin receptors. Int J Parasitol 42:269–277.

 \triangleleft

Infection and Immunity

35. Sun X, Yang F, Shen J, Liu Z, Liang J, Zheng H, Fung M, Wu Z. 2016.
Recombinant Sj16 from *Schistosoma japonicum* contains a functional Nterminal nuclear localization signal necessary for nuclear translocation in
dendritic cells and interleukin-10 production. Parasitol Res 115:4559–4571.

731 36. Frankel AD, Pabo CO. 1988. Cellular uptake of the tat protein from human
732 immunodeficiency virus. Cell 55:1189–1193.

Joliot A, Pernelle C, Deagostini-Bazin H, Prochiantz A. 1991. Antennapedia
homeobox peptide regulates neural morphogenesis. Proc Natl Acad Sci U S A
88:1864–8.

736 38. Fawell S, Seery J, Daikh Y, Moore C, Chen LL, Pepinsky B, Barsoum J. 1994.
737 Tat-mediated delivery of heterologous proteins into cells. Proc Natl Acad Sci U
738 S A 91:664–668.

739 39. Ferrari A, Pellegrini V, Arcangeli C, Fittipaldi A, Giacca M, Beltram F. 2003.
740 Caveolae-mediated internalization of extracellular HIV-1 Tat fusion proteins
741 visualized in real time. Mol Ther 8:284–294.

40. Efthymiadis A, Briggs LJ, Jans DA. 1998. The HIV-1 tat nuclear localization
sequence confers novel nuclear import properties. J Biol Chem 273:1623–
1628.

Kuppuswamy M, Subramanian T, Srinivasan A, Chinnadurai G. 1989. Multiple
functional domains of Tat, the trans-activator of HIV-1, defined by mutational
analysis. Nucleic Acids Res 17:3551–61.

748

749

750 ACKNOWLEDGMENTS

We would like to thank Dr Christian Beetz for the kind donation of the TetraEGFP plasmid and Dr Hilary Collins for help with confocal microscopy. This work was funded by an NIH R56 grant (R56AI119168) awarded to MHH and TSJ. The funders had no role in study design, data collection and interpretation, or the decision to submit the work for publication.

756

757 Figure Legends758

759 760

761 Figure 1: S. haematobium expresses multiple forms of H-IPSE. A) Amino acid 762 763 sequences of predicted H-IPSE paralogs, M-IPSE, and sequenced transcripts from 764 egg cDNA were globally aligned using a Blosum62 cost matrix and a tree was built 765 using the neighbor-joining method in Geneious 7.1.4. Scale bar represents amino acid substitutions per site. H06 and H03 variants chosen for expression are 766 767 highlighted in green, and their respective amino acid identity and identity to M-IPSE 768 are shown. All variants identified through 3' RACE cloning are denoted with asterisks. B) Alignment of amino acid sequences of H03-IPSE (top row) and H06-769 770 IPSE (middle row) with the homolog in S. mansoni (IPSE/alpha-1, named M-IPSE 771 here, bottom row). These H-IPSE clones retain ~63-68% amino acid identity and several previously features described in M-IPSE (20), including: a 20 amino acid 772 773 classical signal sequence, seven cysteine residues involved in disulfide bonds, two 774 N-linked glycosylation consensus motifs, and a predicted nuclear localization 775 sequence (data not shown). Residues colored in green are identical, residues in 776 yellow share properties (e.g. hydrophobicity, polarity), and residues in red lack 777 similarity. C) SDS-PAGE gel (left) and western blot with anti-H06-IPSE antiserum (right). Lanes contain parasite-derived adult worm antigen (AWA), egg secretory 778 779 protein (ESP), or soluble egg antigen (SEA).

780

781

A

Figure 2: Effect of multiple amino acid substitutions on NLS in H-IPSE. A) The 782 783 nucleotides encoding the H03/H06-IPSE nuclear localization sequence (SKRRRKY and SKRGRKY, respectively) were inserted into the pTetra-EGFP construct (2,3). 784 pTetra-EGFP encodes a tetrameric EGFP construct resulting in the expression of a 785 786 fluorescent protein which due to its size (>100 kDa) is excluded from the nucleus in the absence of a functional NLS (Tetra-EGFP) or imported into the nucleus in the 787 presence of a functional NLS (canonical SV40 NLS, H03/H06-IPSE NLS). Nuclei 788 were stained with DAPI and green fluorescence measured with the GFP light cube 789 on an EVOS fl microscope, 24 hours after transfection. Bar is 100 µm. B) 790 791 Comparison of wild-type H06-IPSE, H03-IPSE and H03-IPSE mutant NLS effect on nuclear localisation of Tetra-EGFP fusion protein. One hundred transfected HTB9 792 cells were evaluated under the EVOS fl microscope for each transfection and the 793 percentage of cells displaying exclusive nuclear fluorescence, as opposed to 794 795 cytosolic only or mixed cytosolic/nuclear localization, recorded. Positive control: 796 Sv40 canonical NLS sequence; negative control: unmodified Tetra-EGFP vector 797 (Tetra-EGFP).

798

799	Figure 3: Expression of M-IPSE and H-IPSE in HEK293-6A cells. A) Schematic
800	diagram of pTT5 H03/06-IPSE expression cassette. eCMV=Cytomegalovirus (CMV)
801	enhancer sequence; pCMV=CMV promoter; TPL=tripartite leader sequence from
802	adenovirus; eMLP=enhancer element from the adenovirus major late promoter
803	(MLP); hVEGF=human vascular endothelial growth factor signal sequence;
804	8xHis=octahistidine tag; TEV=Tobacco Etch Virus protease cleavage site; STOP:
805	stop codon; pA: β -globin polyadenylation signal. B) Coomassie-stained 4-20% SDS-
806	PAGE gradient gel and C) Western Blotting of recombinant H03-IPSE (and M-IPSE,
807	used as comparison) expressed in HEK 293SF-3F6 cells and purified by IMAC from
808	serum-free culture supernatant, and run under non-reducing (NR) or reducing (R)
809	conditions.

 $\overline{\triangleleft}$

 $\overline{\mathbf{A}}$

810 Figure 4: Recombinant H03-IPSE is taken up by HTB-9 host cells and translocates 811 to the nucleus. HTB-9 cells, incubated for 24 hours with 0.40 nM recombinant H03-IPSE, were stained with 5 µM DRAQ5 nuclear stain for 15 minutes at room 812 temperature, followed by staining with a mouse anti-His antibody and Alexa Fluor® 813 555 conjugated Goat anti-Mouse IgG (H+L) as secondary antibody. The right column 814 shows the overlay of the two channels. The uptake in HTB-9 cells was visualized by 815 816 confocal microscopy. The primary anti-His antibody was omitted in the control lane.

817

826

827

818

819

820

821

822

823

824

825

Figure 6: Stage-specific expression of H-IPSE mRNA. RT-PCR results for H-IPSE 828 829 obtained from cDNAs, prepared by reverse transcription of DNAse-treated RNA of 830 various life stages of S haematobium. Ladder: 100 basepair (Bp) DNA ladder; egg: S. haematobium egg cDNA; mir: miracidial cDNA; cer: cercarial cDNA; som: in vitro 831 832 mechanically transformed schistosomula cDNA; Ad, F, M mixed cDNA from female, male or mixed adult worms, respectively. ShTub: control housekeeping gene, S. 833 834 haematobium tubulin.

Figure 5: Fluorescence microscopy of HTB-9 cells incubated with recombinant H03-

IPSE (NLS: SKRRRKY), H06-IPSE (NLS: SKRGRKY) or H03-IPSE mutant (NLS:

SKAAAKY). HTB-9 cells were stained with Hoechst 33342 nuclear stain for 15

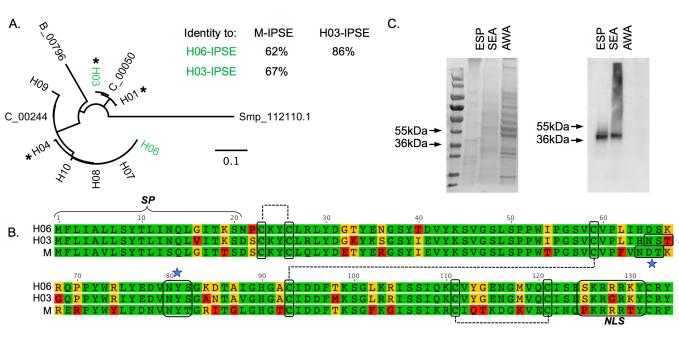
minutes at room temperature, followed by staining with a mouse anti-His antibody

and Alexa Fluor® 555-conjugated Goat anti-Mouse IgG (H+L) as secondary

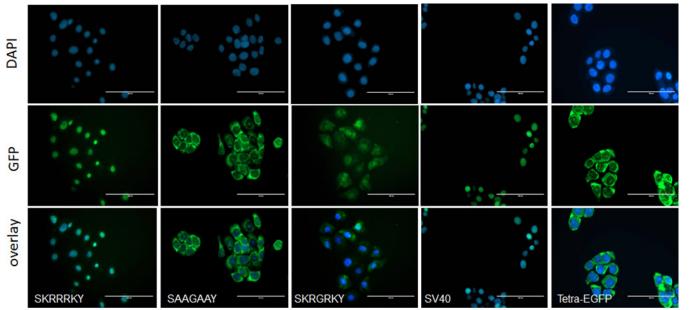
antibody. The right column shows the overlay of the two channels. The primary anti-

His antibody was omitted in the control lane. Bar size is 100 µm.

Downloaded from http://iai.asm.org/ on September 25, 2017 by SERIALS DEPT

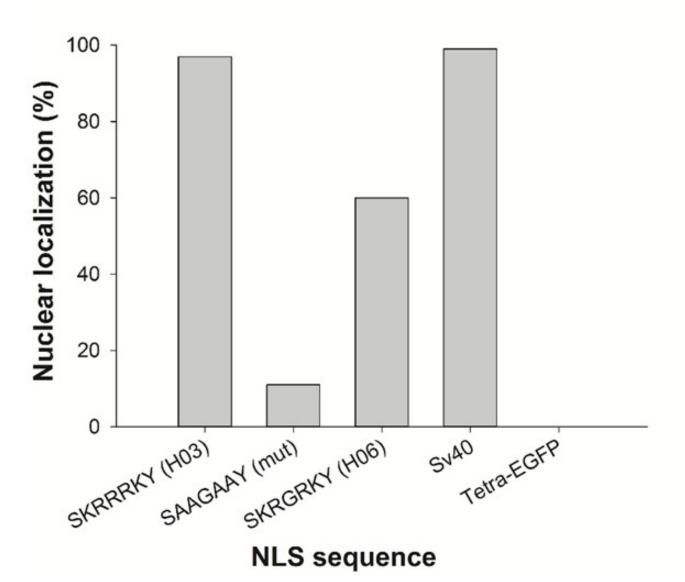


 $\overline{\triangleleft}$



 \mathbb{A}

 $\overline{\mathbb{A}}$



А

В

75

50

37

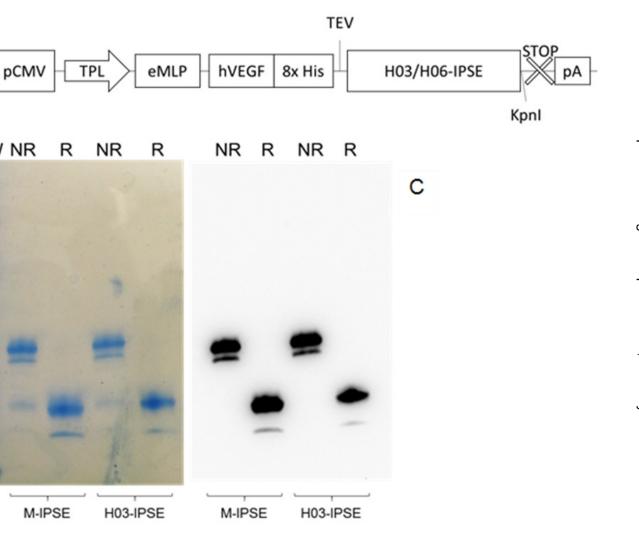
25 20

15

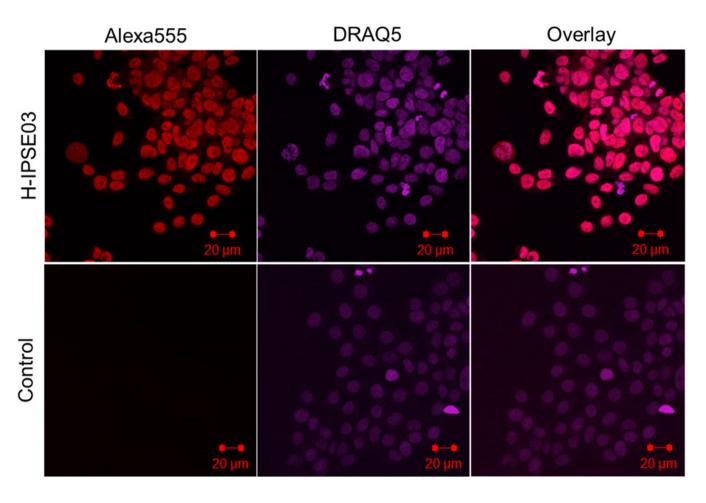
10

eCMV

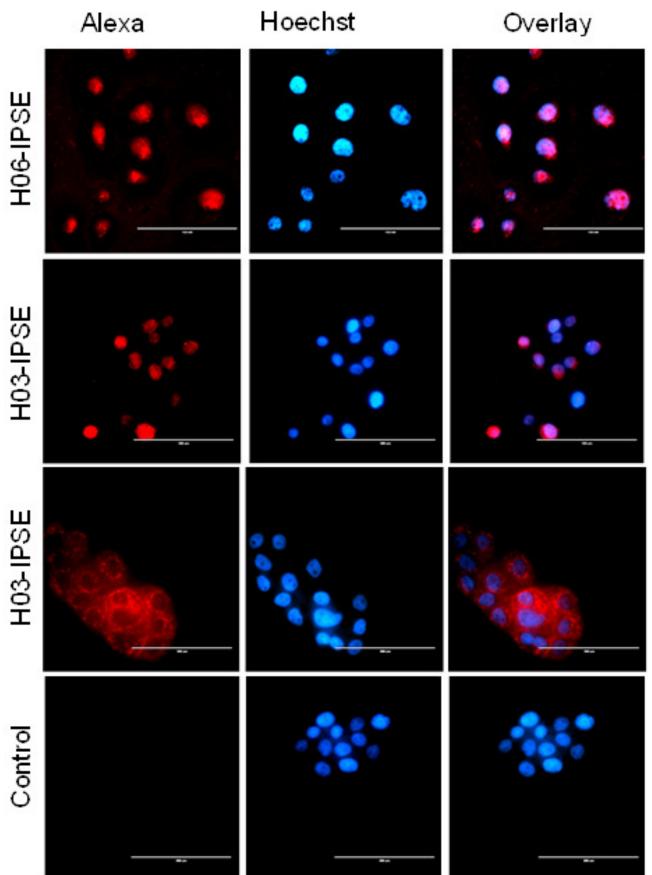
MW NR



Infection and Immunity

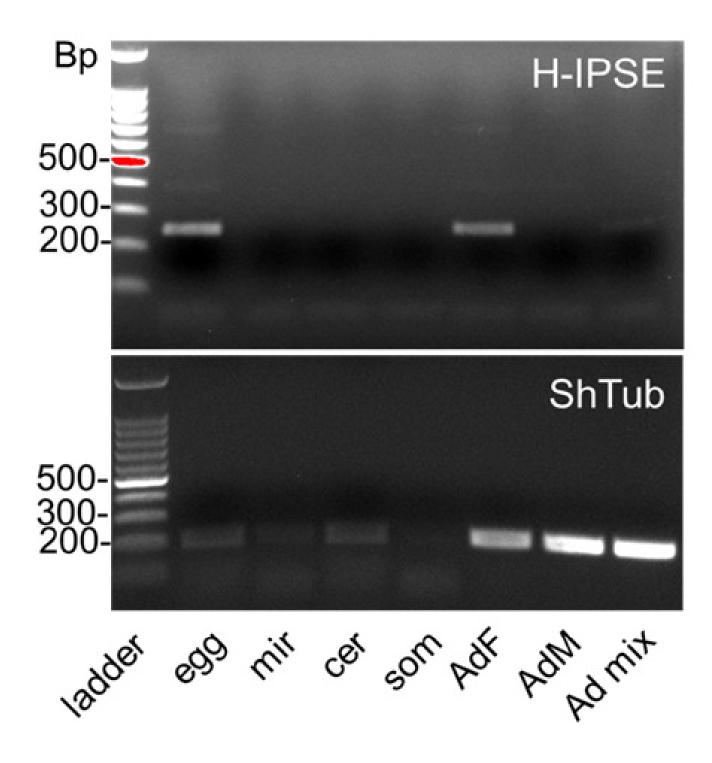


 $\overline{\triangleleft}$



 $\overline{\triangleleft}$

Infection and Immunity



Downloaded from http://iai.asm.org/ on September 25, 2017 by SERIALS DEPT

 $\overline{\mathbb{A}}$